Additive Manufacturing 27 (2019) 318–326

Contents lists available at ScienceDirect

Additive Manufacturing

journal homepage: www.elsevier.com/locate/addma

Full Length Article

One-step electrodeposition of copper on conductive 3D printed objects

Myung Jun Kim[a,1], Mutya A. Cruz[a,1], Shengrong Ye[b], Allen L. Gray[b], Gabriel L. Smith[c], Nathan Lazarus[c], Christopher J. Walker[d], Hjalti H. Sigmarsson[d], Benjamin J. Wiley[a,*]

[a] Department of Chemistry, Duke University, 124 Science Drive, Box 90354, Durham, NC 27708, United States
[b] Multi3D LLC. 101-U Woodwinds Industrial Court, Cary, NC 27511, United States
[c] Army Research Lab, 2800 Powder Mill Rd, Adelphi, MD 20783, United States
[d] Advanced Radar Research Center (ARRC), School of Electrical and Computer Engineering, The University of Oklahoma, Norman, OK 73019, United States

ARTICLE INFO

Keywords:
3D printing
Conductive filament
One-step electrodeposition
Inductive coil
Horn antenna

ABSTRACT

3D printing with electrically conductive filaments enables rapid prototyping and fabrication of electronics, but the performance of such devices can be limited by the fact that the most conductive thermoplastic-based filaments for 3D printing are 3750 times less conductive than copper. This study explores the use of one-step electrodeposition of copper onto electrically conductive 3D printed objects as a way to improve their conductivity and performance. Comparison of three different commercially-available conductive filaments demonstrates that only the most conductive commercially available filament could enable one-step electrodeposition of uniform copper films. Electrodeposition improved the electrical conductivity and the ampacity of 3D printed traces by 94 and 17 times respectively, compared to the as-printed object. The areal surface roughness of the objects was reduced from 9.3 to 6.9 μm after electrodeposition, and a further reduction in surface roughness to 3.9 μm could be achieved through the addition of organic additives to the electrodeposition bath. Copper electrodeposition improved the quality factor of a 3D printed inductor by 1740 times and the gain of a 3D printed horn antenna by 1 dB. One-step electrodeposition is a fast and simple way to improve the conductivity and performance of 3D printed electronic components.

1. Introduction

3D printing enables rapid prototyping of objects, including those with complex structures that cannot be easily produced with traditional subtractive manufacturing processes. [1–3] Among the different methods of 3D printing, fused filament fabrication (FFF), also called fused deposition modeling (FDM), is the most accessible due to the widespread commercial availability of desktop printers that accommodate two standardized filament sizes. In FFF, a thermoplastic filament (most commonly polylactic acid) is fed into a heated nozzle, which extrudes the molten thermoplastic onto a print bed. As the thermoplastic cools after leaving the nozzle, it solidifies, thereby enabling printing of 3D structures. Thermoplastics have been doped with various magnetic or electrically conductive fillers to expand the potential applications of 3D printing. These materials have been used to 3D print magnetic textiles, magnetic transformers, touch sensors, microwave metamaterials, AC radio frequency circuits, wireless power transfer circuits, high-pass filters, and horn antennas. [4–6]

Electrically conductive filaments for FFF have used carbon-based fillers, such as graphite, graphene, and multi-walled carbon nanotubes (MWCNT). [7–12] However, the electrical resistivity of carbon-based filaments is relatively high (1 Ω cm for a MWCNT-based filament [7], 0.8–1.2 Ω cm for a graphene-based PLA filament from Black Magic, and 10.5–12 Ω cm for a carbon black-based PLA filament from Proto-Pasta) [5]. Electrifi, a commercially available filament containing a metallic filler, has a significantly lower electrical resistivity of 0.006 Ω cm. [5]. Cruz et al. have also reported a silver-coated copper nanowire-based conductive filament with an electrical resistivity of 0.002 Ω cm, which is the most conductive filament for FFF reported to date. [13] The improvement in electrical conductivity was due to the anisotropic shape of the nanowires and the intrinsically superior conductivity of metal compared to carbon-based materials [14]. However, the electrical resistivities of Electrifi and the silver-coated copper nanowire-based filament are still 3750 and 1250 times higher than bulk copper (1.67 μΩ cm), respectively, which prevents the utilization of 3D printed objects in applications requiring high electrical conductivity.

One promising method of improving the electrical conductivity of 3D printed objects is through the electrochemical deposition of copper.

* Corresponding author.
E-mail address: benjamin.wiley@duke.edu (B.J. Wiley).
[1] These authors contributed equally to this work.

https://doi.org/10.1016/j.addma.2019.03.016
Received 14 November 2018; Received in revised form 16 January 2019; Accepted 18 March 2019
Available online 19 March 2019
2214-8604/

Electroplating objects made from a non-conductive filament typically involves a surface roughening step, surface activation, electroless deposition, and an electroplating step to obtain a thicker metal film. [15–21] The electroless plating process typically requires an activation step with expensive catalysts prior to electroless plating, and the electroless plating bath is chemically unstable, [22,23] requiring its replacement on a daily basis. If a specific pattern of metal is desired, additional lithographic processes are necessary because electroless deposition will cover all exposed surfaces with metal. Alternatively, one can perform one-step electrodeposition on conductive parts of a 3D printed object with a simple, low-cost, chemically stable electrodeposition bath (e.g. copper sulfate & sulfuric acid). [24] However, the low conductivity of the filament used in previous work necessitated the clamping of copper foil to the printed object < 1 cm from the area onto which copper was deposited, suggesting that this method can be applied only to relatively small parts. In addition, the copper deposit in this previous work was relatively rough. Indeed, the uniformity of electroplated metal can be affected by a voltage drop if the object is not very conductive. [25,26] For example, the thickness of the copper deposit can decrease with distance from the point of electrical contact. [26] This suggests that the relatively high electrical resistivity of the filament material used in previous work prevented the deposition of uniform copper films on 3D printed objects. However, there is no research addressing the effect of electrical resistivity on the uniformity of metal electrodeposition on conductive 3D printed objects.

In this study, we explored how the electrical resistance of 3D printed traces affects one-step electrodeposition of copper on commercially available Electrifi, Black Magic, and Proto-Pasta 3D printing filaments. We observed that electrodeposition of copper on the Black Magic and Proto-Pasta conductive filaments resulted in non-uniform films due to their relatively high electrical resistance. Uniform deposits could be obtained on Electrifi due to its much lower electrical resistivity. We further demonstrate how the addition of organic additives to the electrolyte decreased the linear surface roughness from 6.9 to 3.9 μm and improved the electrical conductivity by 150%. Copper electrodeposition on Electrifi was used to increase the quality factor of a 3D-printed solenoid coil by 1740 times, and increase the gain of a horn antenna by 1 dB, demonstrating its ability to quickly improve the performance of 3D printed electronic components.

2. Methods

2.1. 3D printing and sample preparation

Traces of Electrifi, Black Magic, and Proto-Pasta were printed with a Creality CR-10 3D printer with a 0.4 mm-diameter orifice nozzle at print speeds of 15, 30, and 30 mm/s at print temperatures of 140, 200, 200 °C, respectively (Table 1). The printing conditions were chosen to minimize printing defects. The traces were printed on acrylic substrates (McMaster-Carr 8505K91) as shown in Fig. 1A. The thickness, width, and length of the printed traces were 0.1, 0.5, and 8 cm, respectively. As shown in the schematic in Fig. 1D, the first centimeter of the trace was coated with Ag paste so as to reduce contact resistance when the trace is connected to the power supply. The second centimeter of the trace was covered with a nonconductive epoxy, which defined the interface between air and the electrolyte and prevented the Ag paste from being exposed to the electrolyte. Each printed trace had an electrodeposition area of 4.25 cm^2 (i.e. 6 cm in length). Optical Microscope and SEM images of the surfaces of the traces are shown in Fig. 1B. The inductive coils and horn antennas were printed with Electrifi as described above.

Table 1
Printing Conditions for the Three Filaments Used in this Study.

Filament	Speed	Temperature
Proto-Pasta	30 mm/s	200 °C
Black Magic	30 mm/s	200 °C
Electrifi	15 mm/s	140 °C

2.2. One-step electrodeposition of copper

The experimental setup for copper electrodeposition is shown in Fig. 1C. Copper electrodeposition was performed with a two-electrode system consisting of the printed object as the working electrode and copper foil as the counter electrode. The printed object was immersed in ethanol and sonicated for 60 s to improve surface wettability and to clean the surface prior to copper electrodeposition. An aqueous electrolyte for copper electrodeposition was composed of 1.0 M $CuSO_4$ (VWR), 0.5 M H_2SO_4 (VWR), and 1 mM NaCl (Fisher Chemical). To explore the effect of organic additives on copper electrodeposition, 100 μM Polyethylene glycol (PEG, average MW 3350, Sigma-Aldrich), 20 μM Sodium 3-mercapto-1-propanesulfonate (MPSA, TCI), and 50 μM Janus Green B (JGB, Alfa Aesar) were added to the electrolyte. Copper electrodeposition was carried out by applying a constant current with a DC power supply (KORAD KA3005 P). The current density for the printed traces was fixed at 50 mA/cm^2, and the electrolyte was agitated with a magnetic stirrer at a rotating speed of 300 rpm. The deposition rate of copper at 50 mA/cm^2 was calculated to be 1.1 μm/min with a current efficiency of 100%. Electrodeposition on the printed coil was performed in the same electrolyte with PEG-MPSA-JGB. Step current deposition was used, which consisted of applying 11.3 mA/cm^2 for 20 min followed by 22.6 mA/cm^2 for 160 min. For the electrodeposition on the horn antenna, the outer surface of the as-printed horn was covered with super glue to selectively perform copper electrodeposition inside the horn. Copper electrodeposition was performed at 25 mA/cm^2 for 120 min without organic additives.

2.3. Characterization

Each trace was divided into four sections and the resistance of each section was measured by attaching alligator clips at the points marked with black dotted lines, as shown in Fig. 1D. For the as-printed traces, the resistance was measured after applying Ag paste to eliminate contact resistance. After copper electrodeposition, the alligator clips were directly clamped onto the printed trace without Ag paste. Resistance was calculated from a current-potential line obtained with a Potentiostat (CH Instruments, Inc. CHI600D). The resistance of the alligator clips was subtracted from the measured resistance. Images for printed traces before and after electrodeposition were taken with a bright field optical microscope (ZEISS Axio Lab.A1) and a scanning electron microscope (SEM, FEI XL30 SEM-FEG, Hitachi S-4700) at the positions given in Fig. 1D. Surface roughness was measured with a 3D optical profiler (ZYGO NewView 5000). Mechanical tensile testing of the electroplated Electrifi after soldering was carried out using a microstrain analyzer (TA Instruments RSA III). The inductance and resistance of solenoid coils fabricated via 3D printing before and after copper electrodeposition were measured with an impedance analyzer (Agilent 4924 A).

The performance of the horn antennas was measured in an anechoic chamber. The tests were conducted across the entire Ka-band. The source antenna used was a PE9850-20 Pasternack standard gain horn with a nominal 20 dB of gain and SWC-28KF-R1 WR-28 waveguide adapter. The antenna under test was mounted to a fixture that was placed atop a pedestal that was rotated at a constant speed to record the received signal by the network analyzer as a function of angle. The network analyzer takes the transmitted and received power and represents it in a matrix of scattering parameters (S-parameters), which can then be used to extract the gain and HPBW of the antennas.

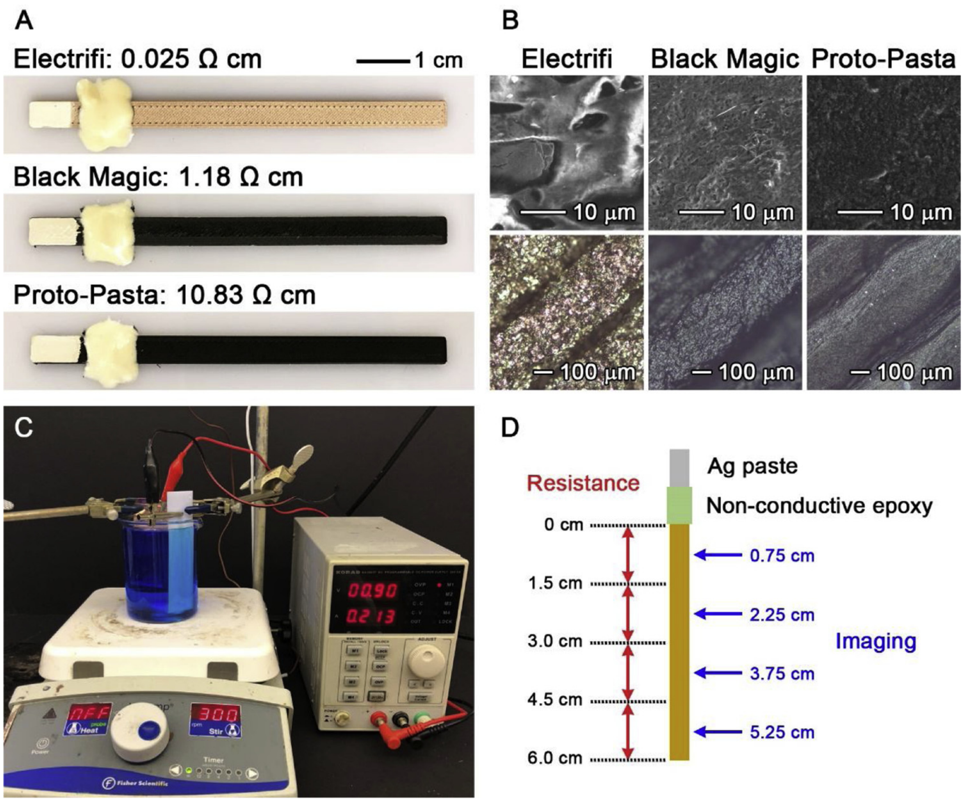

Fig. 1. (A) Printed traces of Electrifi, Black Magic, and Proto-Pasta. (B) SEM (top row) and optical microscope (bottom row) images showing the surface structure of the printed objects. (C) Experimental set-up for copper electrodeposition. (D) Schematic diagram showing the positions where resistance was measured and images were taken.

3. Results and discussion

3.1. One-step electrodeposition on printed traces

We printed linear traces with three commercially available conductive filaments (Electrifi, Black Magic and Proto-Pasta) to investigate the effects of potential drop on one-step electrodeposition of copper. The resistivities of the printed traces were 0.025 Ω cm for Electrifi, 1.18 Ω cm for Black Magic, and 10.83 Ω cm for Proto-Pasta (Fig. 1A). We electroplated copper onto the trace by connecting one end of the trace (covered with Ag paste) to a power supply (Figs. 1A and 1C), and submerging the trace in $CuSO_4$-H_2SO_4 electrolyte to perform galvanostatic copper electrodeposition. The current density for copper electrodeposition was fixed at 50 mA/cm^2 regardless of the filament to control the copper deposition amount and compare the electrical properties for the same amount of deposited copper. In galvanostatic electrodeposition, the potential is higher near the electrical contact, resulting in a thicker copper deposit in this region. The potential gradually decreases as the distance increases between the electrical contact and the region where electrodeposition takes place (i.e. the potential drops along the printed trace), leading to the least amount of copper deposited at the area furthest from the electrical contact. Since the potential drop increases with the resistance of the substrate, [25,26] a higher electrical resistance can result in non-uniform electrodeposition.

The results of copper electrodeposition on the linear traces printed with the Proto-Pasta, Black Magic, and Electrifi filaments are presented in Figs. 2 and 3. Electrifi had the most uniform copper electrodeposits, followed by Black Magic, and finally Proto-Pasta. Thus, the uniformity of the electroplated copper directly correlated with the conductivity of the filament.

For the least conductive Proto-Pasta trace, Figs. 2A and 3 A show a continuous copper film was obtained only within 2 cm from the electrical contact even after 1 h of copper electrodeposition. At the maximum voltage of the power supply (30 V), the maximum current density that could be obtained during plating was 2.59–2.92 mA/cm^2 due to the high resistance of the Proto-Pasta trace. As a result of the severe potential drop and low current density, a small amount of copper electrodeposition took place only near the electrical contact, with a few small copper particles deposited at the end of the trace (Fig. 3A). The non-uniform copper electrodeposition led to a large variation in the electrical resistance along the length, ranging from 210 to 1000 Ω after 1 h of copper electrodeposition. Copper electrodeposition decreased the resistance only near the electrical contact from 490 Ω (at 5 min) to 213 Ω (at 1 h).

The Black Magic filament was able to act as a substrate for one-step copper electrodeposition, but the deposition was not uniform due to the relatively low conductivity of the filament. Figs. 2B and 3 B show the propagation of copper growth from the electrical contact to the end of the trace. After 5 min, copper was concentrated near the electrical contact, and full coverage of the trace was only achieved after 60 min. The non-uniform nature of the copper film on Black Magic could also be observed with measurements of electrical resistance along the trace (Fig. 2B). The concentration of electroplated copper near the electrical contact led to a preferential decrease in the resistance in that region. Even after 1 h of copper electrodeposition, the resistance between 0 and 1.5 cm was 6.8 times lower than that between 4.5 and 6 cm from the point of electrical contact.

The electrodeposition of copper on the Electrifi trace resulted in a uniform film when examined by eye (Fig. 2C). However, optical microscope and SEM (Fig. 3C) images showed that the coverage of copper on the Electrifi trace was not perfectly uniform. After electrodeposition for 5 min, more copper deposited near the electrical contact, and overall the electroplated copper was patchy and discontinuous. After 15 min, larger continuous patches formed. After 30 min, almost the entire Electrifi surface was covered with copper, with rare, sporadic voids observed. Electrodeposition for 1 h resulted in the formation of a completely continuous copper film. The change in the resistance of the Electrifi trace as a function of deposition time and position is shown in Fig. 2C. Since the trace with an electrodeposition time of 5 min was not completely covered by copper deposits, its resistance was higher than

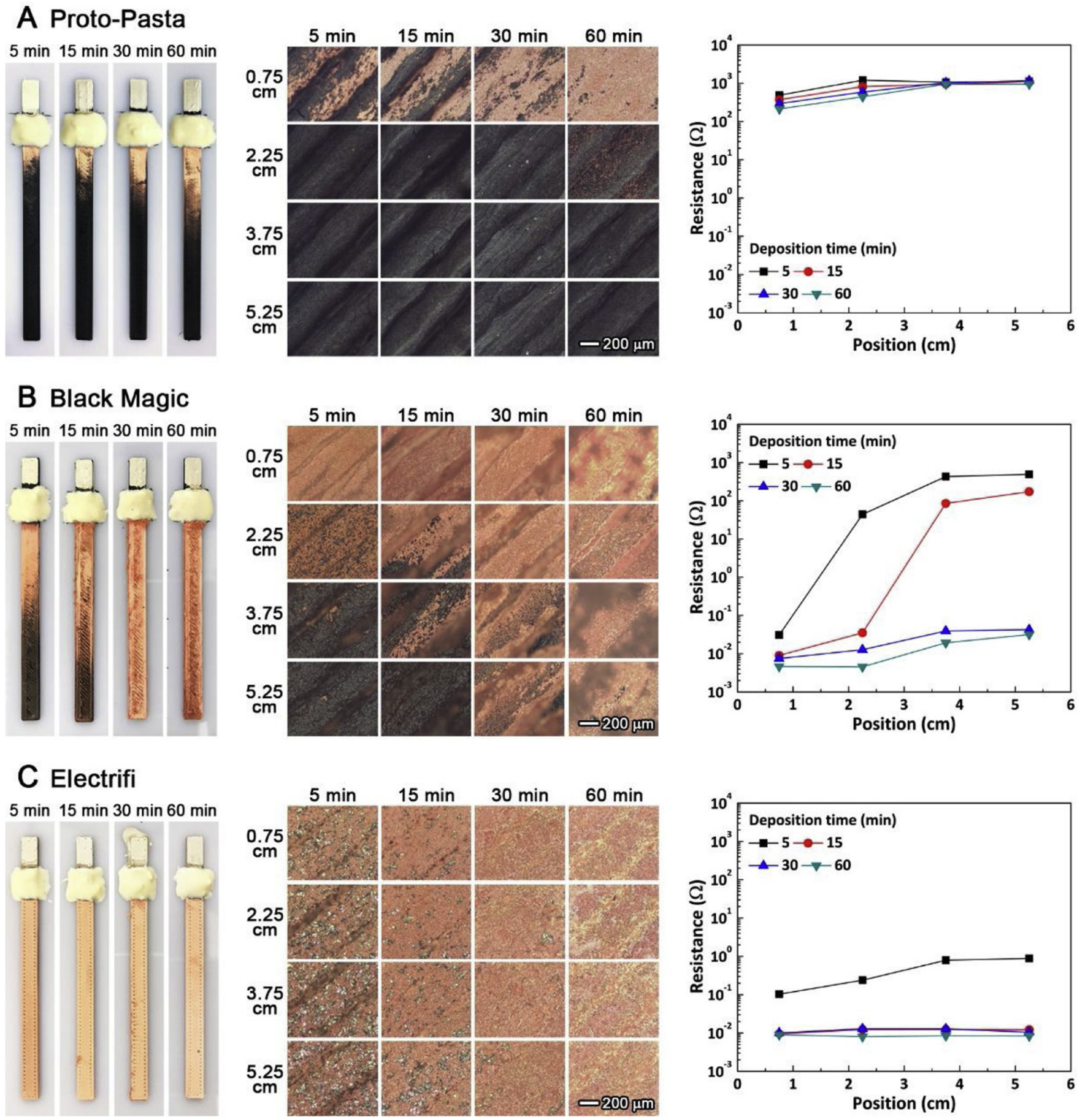

Fig. 2. Pictures, optical microscope images, and the corresponding resistances of 3D printed (A) Proto-Pasta, (B) Black Magic, and Electrifi traces after copper electrodeposition.

0.100 Ω for all four testing points along the trace. The resistance near the point of electrical contact was lower than the resistance at the end of the trace due to more deposition of copper near the electrical contact. After electrodeposition for > 15 min, the resistance values were all below 0.025 Ω and were uniform along the length of the trace. Although an electrodeposition time of 15 min resulted in a trace with voids (exposed thermoplastic), its electrical resistance was low due to the formation of a continuous path of copper.

Thus, the low resistivity of Electrifi resulted in the most uniform copper electrodeposition. Copper electrodeposition was uniform even on a 1 mm-wide trace (Figure S1), which had a resistance 5 times higher than the 5 mm-wide traces. However, SEM images showed the copper deposits were relatively rough with a few pores, which can increase the resistance of the films. To address this issue, we investigated whether the uniformity of the copper film could be improved by adding organic additives into the electrolyte.

3.2. The effect of organic additives on one-step copper electrodeposition

Organic additives are commonly used to promote defect-free filling of copper in trenches and vias to form interconnects in integrated circuits. [27–33] Organic additives can also promote the deposition of a smooth copper film through a process referred to as leveling. [34] Leveling is a phenomena in which organic additives preferentially adsorb on convex regions in a film and selectively inhibit copper deposition, resulting in copper electrodeposition occurring to a greater extent in concave regions, and a corresponding decrease in surface roughness.

Figs. 4A and S2 show SEM images of copper deposited with and without the additive combination of PEG-MPSA-JGB, a common combination used for leveling. [34] Crevices between adjacent copper protrusions were clearly present in the images of copper deposited without additives (the left images in Fig. 4A). The addition of PEG-MPSA-JGB dramatically smoothed the surface of the copper deposits, resulting in a film in which no boundaries between protrusions could be observed. In addition, Figure S2 illustrates that the pores in the copper film that were observed without additives at 30 min were absent after adding additives to the deposition solution. These results indicate the additives promoted the lateral growth of copper while inhibiting vertical growth, leading to a smoother copper film.

The effect of the organic additives on the surface roughness of

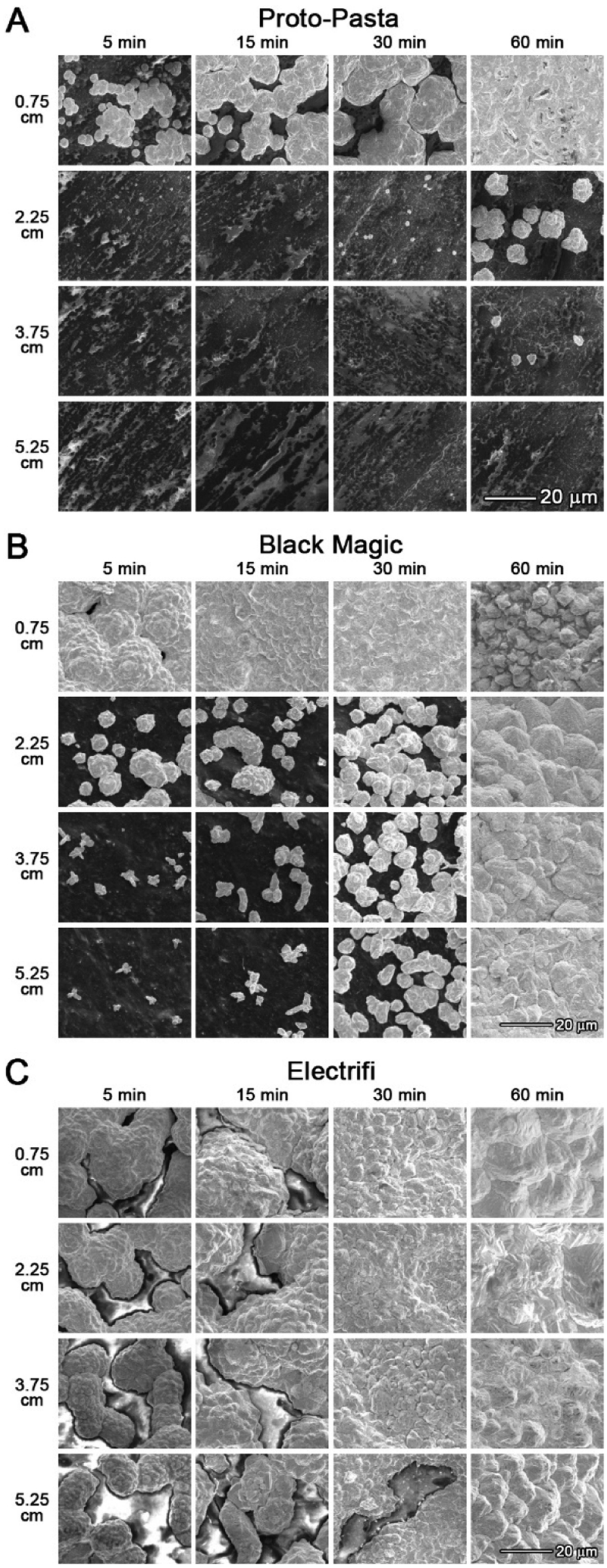

Fig. 3. SEM images of 3D printed (A) Proto-Pasta, (B) Black Magic, and (C) Electrifi traces at different positions and electrodeposition times.

copper deposits was further measured with 3D optical profiling. Figs. 4B-D shows the optical profiling images of Electrifi before copper deposition, after copper deposition without additives, and after copper deposition with additives. The areal RMS roughness (R_A) was calculated from the image as a whole, and the linear RMS roughness (R_L) was obtained from the morphology of the copper along the printed line as described in Fig. 4B. The R_A for the as-printed Electrifi was around 14.1 μm, which decreased to 8.9 μm after copper electrodeposition without organic additives, and 7.3 μm with organic additives. The linear RMS roughness also decreased from 9.3 μm to 6.9 (without additives) and 3.9 μm (with additives). Copper electrodeposition in the presence of organic additives smoothed the surface of the printed object, filled the gaps between the printed lines, and eliminated the boundaries between copper deposits, resulting in decreased linear and areal roughness.

The use of organic additives for copper electrodeposition can decrease the grain size and increase the amount of incorporated impurities, resulting in lower conductivity. [28,35–39] Fig. 5 shows, however, that the resistivity of copper deposited with the organic additives (266 μΩ cm) was 1.5 times lower than the copper deposited without organic additives, and 94 times lower than the as-printed trace. This result suggests that the reduction of surface roughness decreased the electrical resistance of the copper deposits to a greater extent than any increase in resistance caused by decreased grain size or increased impurities. That is, the organic additives facilitated the filling of gaps between copper protrusions, reduced the surface roughness, and increased the surface coverage of copper, leading to a decrease in the electrical resistance for the same amount of deposited copper.

3.3. Ampacity of as-printed and electroplated traces

The use of 3D printing to fabricate electrical interconnects is limited to applications requiring a low current. It was previously reported that even the most electrically-conductive nanowire-based filament suffered from Joule heating, and that the maximum current density of a printed trace was related to its surface area-to-volume ratio. [13] The temperature rise was greatest in the middle of the printed trace, and caused the trace to disconnect from the leads due to the melting of the polymer. A metal coating can reduce Joule heating due to its increased electrical and thermal conductivity. Fig. 6 shows the temperature in the middle of printed traces as the current was increased. For each increase in the current density, the surface temperature gradually increased before reaching a plateau at currents below 0.3 A. At a current of 0.4 A, the surface temperature sharply increased from 33 °C to over 40 °C before the polymer melted and electrical contact with the power supply was lost. Thus, the ampacity of the as-printed trace was 0.3 A. After electrodeposition with organic additives, the trace exhibited an ampacity of 5 A, and a negligible temperature increase (< 5 °C) at currents below 1 A. This current was the maximum that could be supplied with our power supply, and represents a current density of 100 A/cm^2. We did not attempt higher current densities due to safety concerns. Thus, the ampacity for the electroplated trace is at least 16.7 times larger than that of the as-printed trace.

3.4. Soldering

The preferred method of making an electrical contact between two objects is soldering due to its low electrical resistance, high mechanical strength, and convenience. Unfortunately, Electrifi filament and other similar conductive filaments melt at temperatures necessary for soldering, making it necessary to use silver paste or mechanical compression to make contact. However, electrodeposition with copper made it easy to form electrical connections with solder. Figs. 7A and B show examples of attempts to solder to a printed trace before and after electrodeposition. As expected, the Electrifi filament melted as a result of the soldering attempt, but no melting was observed for the

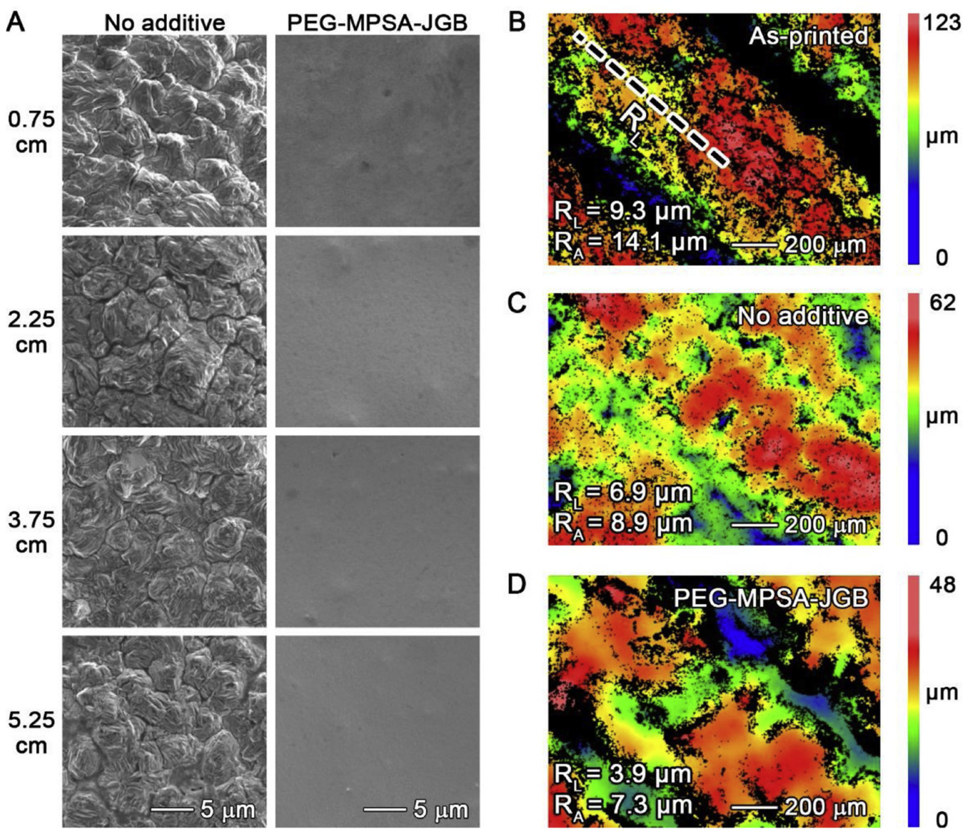

Fig. 4. (A) Top-view images of copper deposited on Electrifi without (left) and with (right) organic additives. 3D optical profiling shows the areal (R_A) and linear (R_L) RMS roughness of (B) Electrifi, (C) Electrifi after copper electrodeposition, and (D) Electrifi after copper electrodeposition with organic additives. The electrodeposition was performed at 50 mA/cm^2 for 30 min.

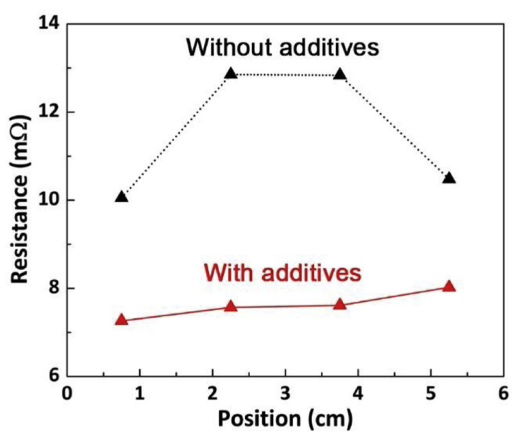

Fig. 5. Resistance of Electrifi traces after copper electrodeposition for 30 min with and without organic additives.

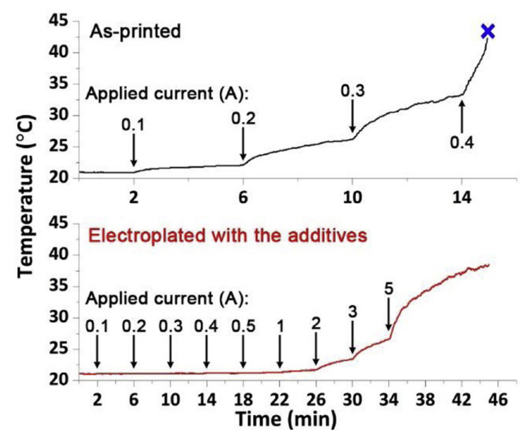

Fig. 6. Temperature change at the middle of 6 cm-long traces with a width of 0.5 cm and a thickness of 0.1 cm as a function of time and increasing current. The electrodeposition condition was 50 mA/cm^2 for 30 min. The failure of the as-printed trace due to Joule heating is marked with an ×, which corresponded to a current density of 8 A/cm^2. The electroplated trace did not fail below the 5 A current limit of the power supply, which corresponded to a current density of 100 A/cm^2.

electroplated trace. The resistance of the solder joint was 0.42 Ω. To test the strength of the solder joint, the ends of the printed trace and the soldered copper wire were clamped to a micro-strain analyzer (Fig. 7C) and a tensile force ramp was applied. The electroplated Electrifi trace fractured before the solder joint, demonstrating that the strength of the joint is greater than that of the trace itself. The ability to solder directly onto the electroplated trace shows that the electroplated copper protected the polymer composite from melting during soldering. Moreover, the solder joint is mechanically strong and has a low electrical resistance. The ability to directly solder to 3D printed electrical components greatly facilitates their integration with components manufactured with traditional processes.

3.5. Electrodeposition of 3D printed inductive coil and horn antenna

Multi-material 3D printing with non-conductive and conductive filaments is a one-step process that is advantageous for 3D printing electrical components and circuits such as inductors, capacitors, and high pass-filters, [5] and can be used to selectively define regions for metal electrodeposition [24]. For example, Fig. 8A shows inductive coils after printing and electrodeposition. The conductive coil was printed with Electrifi and non-conductive black PLA. Electrodeposition took place selectively on Electrifi, resulting in the formation of a shiny copper film, and a 100-fold decrease in the electrical resistance

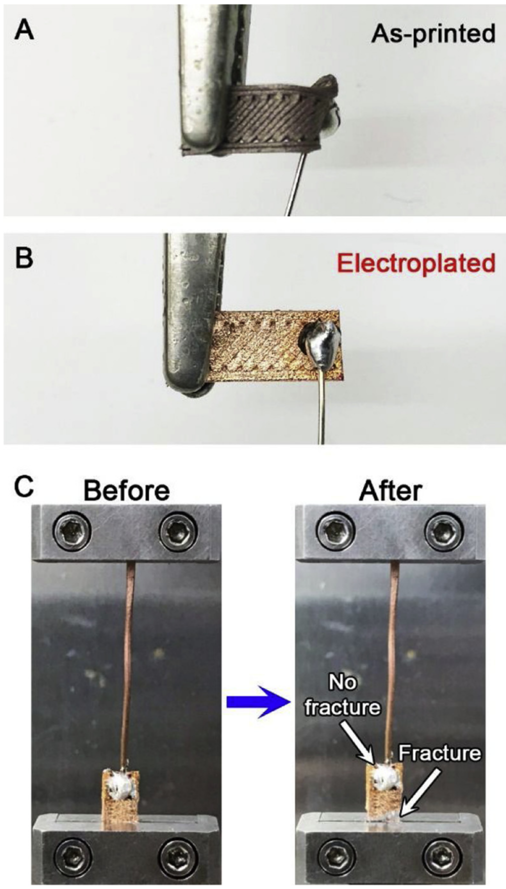

Fig. 7. Pictures of (A) as-printed and (B) electroplated traces after soldering. (C) The electroplated Electrifi trace fractured before the solder joint in a tensile test.

(Fig. 8B). Fig. 8C shows the as-printed coil had a noisy inductance at frequencies below 100 kHz because the electrical resistance was large relative to the inductance, which makes the impedance measurement inaccurate. A stable inductance of 80 nH was observed at frequencies between 10 kHz and 3 MHz. The electroplated coil exhibited a stable inductance throughout the entire frequency range, with an average inductance of 117 nH between a frequency range of 10 kHz to 3 MHz. The quality factor of the electroplated inductor at 1 MHz was 13.7 versus 7.87×10^{-3} for the as-printed coil [40]. This means that the electroplated coil stores energy 1740 times more efficiently than the as-printed coil.

Fig. 9A shows another example of a 3D printed horn antenna coated by copper with one-step electrodeposition. The model was based on a commercially available, PE9850-10 standard gain horn antenna from Pasternack, but slightly modified to remove the extended waveguide. Since the antenna was modified, it was necessary to simulate it using ANSYS HFSS to capture its baseline performance for reference. The simulation showed a gain of 10.7 dB with a half-power beam width (HPBW) of 52.18° at 30 GHz. The outer surface of the horn antenna before electrodeposition was masked with super glue to limit copper electrodeposition to the inner surface of the antenna. The measured radiation patterns for the horn antenna before electrodeposition is shown in Fig. 9B, and that of the electroplated horn antenna without organic additives is shown in Fig. 9C. The measured gain of the horn antennas at 30 GHz was 9.3 dB for the as-printed antenna, and 10.3 dB for the electroplated antenna. The electroplated antenna exhibited a consistent improvement in gain by an average of + 1 dB across the Ka-band frequency band (26.5–40 GHz), as well as a slight increase in half power beam width (HPBW) from 51.2° to 53° at 30 GHz. The improvement in gain and HPBW observed for the electroplated antenna was attributed to an increase in the conductivity and a decrease in the surface roughness achieved with copper electrodeposition. The performance of the electroplated antenna is only 0.4 dB less than the simulated gain, which utilizes bulk copper conductivity and does not include any surface roughness. Furthermore, this implies that the performance of 3D printed horn antennas at higher frequencies, where material conductivity and surface roughness have a more significant effect on gain and HPBW, can also be improved with one-step electrodeposition of copper.

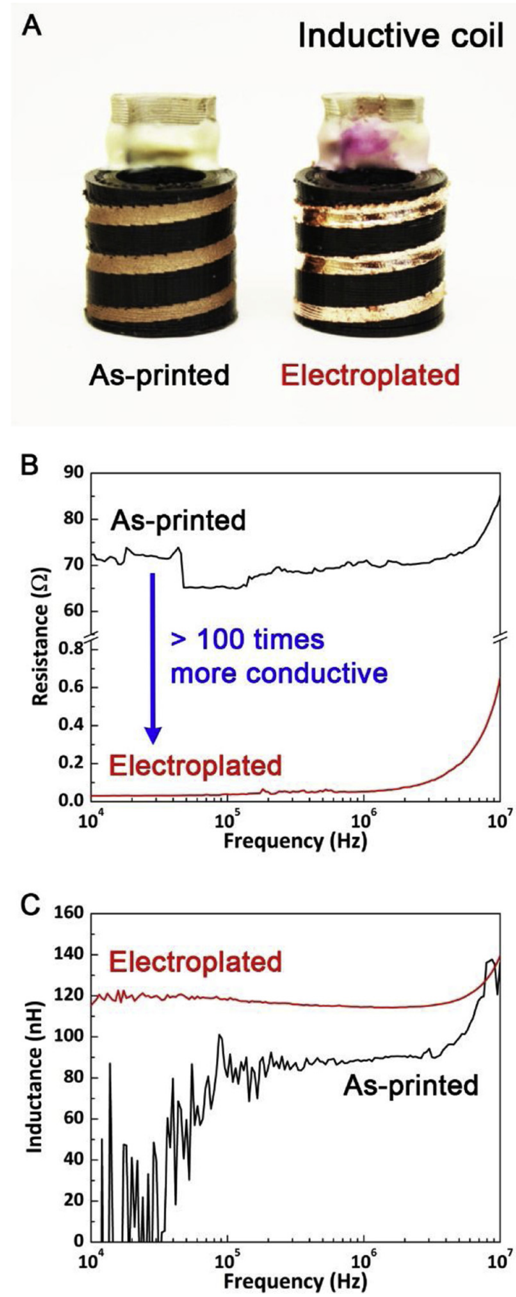

Fig. 8. (A) As-printed and electroplated inductive coils. (B) Electrical resistance and (C) inductance of as-printed and electroplated coils.

4. Conclusions

This study demonstrates a method for fabricating highly conductive 3D structures using FFF 3D printing followed by one-step

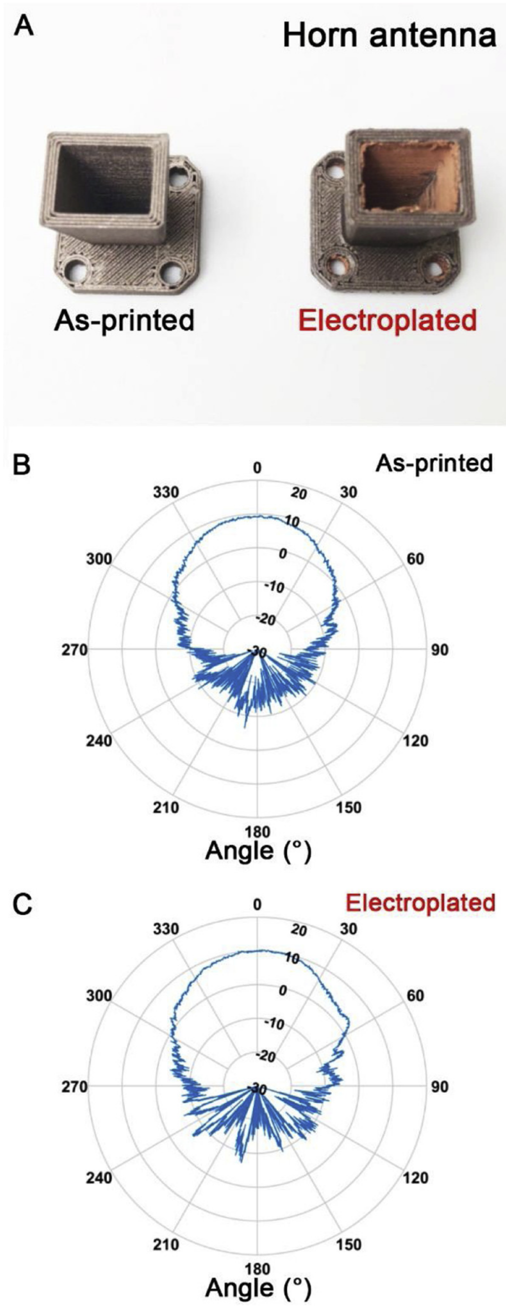

Fig. 9. (A) A picture of as-printed and electroplated horn antennas without organic additives. The radiation patterns at 30 GHz of (B) as-printed and (C) electroplated horn antennas.

electrodeposition of copper. We found that of the three conductive printing materials that are commercially available, only Electrifi was conductive enough to enable the electrodeposition of relatively uniform copper films over several centimeters. The addition of organic additives in the electrolyte further decreased the roughness of the electroplated copper by 77%, and decreased the resistance by 150%. One-step electrodeposition of copper on Electrifi traces reduced their electrical resistance by 94 times, improved their thermal stability, made them solderable, and increased the ampacity of the traces from 8 to 100 A/cm^2. Moreover, one-step electrodeposition can deposit copper in selected (i.e. conductive) areas without the need for lithography. This work will be helpful to those seeking to find a fast and simple way to selectively deposit uniform films of metal on 3D printed parts. For example, the high cost, three-dimensional configuration, and compatible dimensions of antennas make such components an attractive target for further application of this technique. The thermal stability of the plated filaments indicates customized heat spreaders and heat sinks may also now be produced with this method. A similar approach can be applied to electrochemically-compatible metals to fabricate, for example, flow-through 3D electrodes for electrochemical processes. [41,42]

5. Notes

S.Y., A.L.G. and B.J.W. have an equity interest in Multi3D LLC, the manufacturer of Electrifi filament. M.J.K., M.A.C., and B.J.W. designed this project, M.J.K. and M.A.C. conducted copper electrodeposition experiments and analyzed the electrodeposition results, G.L.S. and N.L.C. analyzed the performance of the inductive coils, and C.J.W. and H.H.S. analyzed the performance of the horn antennas. S.Y. and A.L.G. provided the 3D printed samples for electrodeposition. All of the electroplating experiments and characterization was performed by individuals who have no equity interest in or employment by Multi3D LLC.

Acknowledgments

This work was supported in part by a National Science Foundation CAREER award number DMR-1253534 (M.J.K., M.A.C., B.J.W), by a National Science Foundation STTR Phase I Grant, 1721644 (S.Y., A.L.G.), and by the Department of Energy's Kansas City National Security Campus, operated by Honeywell Federal Manufacturing & Technologies, LLC under contract number DE-NA0002839 (C.J.W., H.H.S.). We thank G. Huff and his group for their help measuring the performance of the horn antennas at Texas A&M University.

Appendix A. Supplementary data

Supplementary material related to this article can be found, in the online version, at doi:https://doi.org/10.1016/j.addma.2019.03.016.

References

[1] D. Espalin, D.W. Muse, E. MacDonald, R.B. Wicker, 3D Printing multifunctionality: structures with electronics, Int. J. Adv. Manuf. Technol. 72 (2014) 963–978, https://doi.org/10.1007/s00170-014-5717-7.

[2] H. Bikas, P. Stavropoulos, G. Chryssolouris, Additive manufacturing methods and modeling approaches: a critical review, Int. J. Adv. Manuf. Technol. 83 (2016) 389–405, https://doi.org/10.1007/s00170-015-7576-2.

[3] A. Ambrosi, M. Pumera, 3D-printing technologies for electrochemical applications, Chem. Soc. Rev. 45 (2016) 2740–2755, https://doi.org/10.1039/c5cs00714c.

[4] S.J. Leigh, R.J. Bradley, C.P. Purssell, D.R. Billson, D.A. Hutchins, A simple, low-cost conductive composite material for 3D printing of electronic sensors, PLoS One 7 (2012) e49365, https://doi.org/10.1371/journal.pone.0049365.

[5] P.F. Flowers, C. Reyes, S. Ye, M.J. Kim, B.J. Wiley, 3D printing electronic components and circuits with conductive thermoplastic filament, Addit. Manuf. 18 (2017) 156–163, https://doi.org/10.1016/j.addma.2017.10.002.

[6] Y. Xie, S. Ye, C. Reyes, P. Sithikong, B.I. Popa, B.J. Wiley, S.A. Cummer, Microwave metamaterials made by fused deposition 3D printing of a highly conductive copper-based filament, Appl. Phys. Lett. 110 (2017) 181903, https://doi.org/10.1063/1.4982718.

[7] G. Postiglione, G. Natale, G. Griffini, M. Levi, S. Turri, Conductive 3D micro-structures by direct 3D printing of polymer/carbon nanotube nanocomposites via liquid deposition modeling, Compos. Part A Appl. Sci. Manuf. 76 (2015) 110–114, https://doi.org/10.1016/j.compositesa.2015.05.014.

[8] X. Wei, D. Li, W. Jiang, Z. Gu, X. Wang, Z. Zhang, Z. Sun, 3D printable graphene composite, Sci. Rep. 5 (2015) 11181, https://doi.org/10.1038/srep11181.

[9] D. Zhang, B. Chi, B. Li, Z. Gao, Y. Du, J. Guo, J. Wei, Fabrication of highly conductive graphene flexible circuits by 3D printing, Synth. Met. 217 (2016) 79–86, https://doi.org/10.1016/j.synthmet.2016.03.014.

[10] G. Gonzalez, A. Chiappone, I. Roppolo, E. Fantino, V. Bertana, F. Perrucci, L. Scaltrito, F. Pirri, M. Sangermano, Development of 3D printable formulations containing CNT with enhanced electrical properties, Polymer. 109 (2017) 246–253, https://doi.org/10.1016/j.polymer.2016.12.051.

[11] Q. Mu, L. Wang, C.K. Dunn, X. Kuang, F. Duan, Z. Zhang, H.J. Qi, T. Wang, Digital light processing 3D printing of conductive complex structures, Addit. Manuf. 18 (2017) 74–83, https://doi.org/10.1016/j.addma.2017.08.011.

[12] K. Gnanasekaran, T. Heijmans, S. van Bennekom, H. Woldhuis, S. Wijnia, G. de With, H. Friedrich, 3D printing of CNT- and graphene-based conductive polymer

nanocomposites by fused deposition modeling, Appl. Mater. Today 9 (2017) 21–28, https://doi.org/10.1016/j.apmt.2017.04.003.
[13] M.A. Cruz, S. Ye, M.J. Kim, C. Reyes, F. Yang, P.F. Flowers, B.J. Wiley, Multigram synthesis of Cu-Ag core–shell nanowires enables the production of a highly conductive polymer filament for 3D printing electronics, Part. Part. Syst. Charact. 35 (2018) 1700385, , https://doi.org/10.1002/ppsc.201700385.
[14] I.E. Stewart, M.J. Kim, B.J. Wiley, Effect of morphology on the electrical resistivity of silver nanostructure films, ACS Appl. Mater. Interfaces 9 (2017) 1870–1879, https://doi.org/10.1021/acsami.6b12289.
[15] H. Seong, S.-C. Kim, D.J. Choi, J.-Y. Lee, Y.-J. Ko, S. Yoon, M. Seo, Y.-H. Kim, Effects of bath composition on the adhesion characteristics of electroless Cu layers on epoxy-based polymer substrates, J. Electrochem. Soc. 163 (2016) D250–D255, https://doi.org/10.1149/2.0721606jes.
[16] S.-C. Kim, H. Seong, K. Ahn, D.J. Choi, J.-Y. Lee, Y.-J. Ko, S. Yoon, M. Seo, Y.-H. Kim, A peel adhesion study of electroless Cu layers on polymer substrates, J. Adhes. 94 (2018) 1–14, https://doi.org/10.1080/00218464.2016.1219950.
[17] C.G. Jones, B.E. Mills, R.K. Nishimoto, D.B. Robinson, Electroless deposition of palladium on macroscopic 3D-printed polymers with dense microlattice architectures for development of multifunctional composite materials, J. Electrochem. Soc. 164 (2017) D867–D874, https://doi.org/10.1149/2.1341713jes.
[18] R. Bernasconi, C. Credi, M. Tironi, M. Levi, L. Magagnin, Electroless metallization of stereolithographic photocurable resins for 3D printing of functional microdevices, J. Electrochem. Soc. 164 (2017) B3059–B3066, https://doi.org/10.1149/2.0081705jes.
[19] R. Bernasconi, F. Cuneo, E. Carrara, G. Chatzipirpiridis, M. Hoop, X. Chen, B.J. Nelson, S. Pané, C. Credi, M. Levi, L. Magagnin, Hard-magnetic cell microscaffolds from electroless coated 3D printed architectures, Mater. Horizons 5 (2018) 699–707, https://doi.org/10.1039/c8mh00206a.
[20] S. Olivera, H.B. Muralidhara, K. Venkatesh, K. Gopalakrishna, C.S. Vivek, Plating on acrylonitrile–butadiene–styrene (ABS) plastic: a review, J. Mater. Sci. 51 (2016) 3657–3674, https://doi.org/10.1007/s10853-015-9668-7.
[21] Y. Yu, C. Yan, Z. Zheng, Polymer-assisted metal deposition (PAMD): a full-solution strategy for flexible, stretchable, compressible, and wearable metal conductors, Adv. Mater. 26 (2014) 5508–5516, https://doi.org/10.1002/adma.201305558.
[22] F. Hanna, Z. Abdel Hamid, A. Abdel Aal, Controlling factors affecting the stability and rate of electroless copper plating, Mater. Lett. 58 (2004) 104–109, https://doi.org/10.1016/S0167-577X(03)00424-5.
[23] H.-C. Koo, J.J. Kim, Effects of stabilizing agents on film properties in Ag electroless plating, J. Electrochem. Soc. 155 (2008) D176–D180, https://doi.org/10.1149/1.2823740.
[24] K. Angel, H.H. Tsang, S.S. Bedair, G.L. Smith, N. Lazarus, Selective electroplating of 3D printed parts, Addit. Manuf. 20 (2018) 164–172, https://doi.org/10.1016/j.addma.2018.01.006.
[25] T.O. Drews, S. Krishnan, J.C. Alameda, D. Gannon, R.D. Braatz, R.C. Alkire, Multiscale simulations of copper electrodeposition onto a resistive substrate, IBM J. Res. Dev. 49 (2005) 49–63, https://doi.org/10.1147/rd.491.0049.
[26] L. Yang, T. Atanasova, A. Radisic, J. Deconinck, A.C. West, P. Vereecken, Wafer-scale Cu plating uniformity on thin Cu seed layers, Electrochim. Acta 104 (2013) 242–248, https://doi.org/10.1016/j.electacta.2013.04.094.
[27] T.P. Moffat, J.E. Bonevich, W.H. Huber, A. Stanishevsky, D.R. Kelly, G.R. Stafford, D. Josell, Superconformal electrodeposition of copper in 500–90 nm features, J. Electrochem. Soc. 147 (2000) 4524–4535, https://doi.org/10.1149/1.1394096.
[28] J.B. Marro, C.A. Okoro, Y.S. Obeng, K.C. Richardson, The impact of organic additives on copper trench microstructure, J. Electrochem. Soc. 164 (2017) D543–D550, https://doi.org/10.1149/2.1131707jes.
[29] T.P. Moffat, D. Josell, Extreme bottom-up superfilling of through-silicon-Vias by damascene processing: suppressor disruption, positive feedback and turing patterns, J. Electrochem. Soc. 159 (2012) D208–D216, https://doi.org/10.1149/2.040204jes.
[30] M.J. Kim, Y. Seo, H.C. Kim, Y. Lee, S. Choe, Y.G. Kim, S.K. Cho, J.J. Kim, Galvanostatic bottom-up filling of TSV-like trenches: choline-based leveler containing two quaternary ammoniums, Electrochim. Acta 163 (2015) 174–181, https://doi.org/10.1016/j.electacta.2015.02.173.
[31] M.J. Kim, H.C. Kim, J.J. Kim, The influences of iodide ion on Cu electrodeposition and TSV filling, J. Electrochem. Soc. 163 (2016) D434–D441, https://doi.org/10.1149/2.1111608jes.
[32] W.-P. Dow, M.-Y. Yen, W.-B. Lin, S.-W. Ho, Influence of molecular weight of polyethylene glycol on microvia filling by copper electroplating, J. Electrochem. Soc. 152 (2005) C769–C775, https://doi.org/10.1149/1.2052019.
[33] W.-P. Dow, H.-H. Chen, M.-Y. Yen, W.-H. Chen, K.-H. Hsu, P.-Y. Chuang, H. Ishizuka, N. Sakagawa, R. Kimizuka, Through-hole filling by copper electroplating, J. Electrochem. Soc. 155 (2008) D750–D757, https://doi.org/10.1149/1.2988134.
[34] J.J. Kelly, C. Tian, A.C. West, Leveling and microstructural effects of additives for copper electrodeposition, J. Electrochem. Soc. 146 (1999) 2540–2545, https://doi.org/10.1149/1.1391968.
[35] D. Josell, S.H. Brongersma, Z. Tőkei, Size-dependent resistivity in nanoscale interconnects, Annu. Rev. Mater. Res. 39 (2009) 231–254, https://doi.org/10.1146/annurev-matsci-082908-145415.
[36] A.F. Mayadas, M. Shatzkes, Electrical-resistivity model for polycrystalline films: the case of arbitrary reflection at external surfaces, Phys. Rev. B 1 (1970) 1382–1389, https://doi.org/10.1103/PhysRevB.1.1382.
[37] S.M. Rossnagel, T.S. Kuan, Alteration of Cu conductivity in the size effect regime, J. Vac. Sci. Technol. B 22 (2004) 240–247, https://doi.org/10.1116/1.1642639.
[38] J.J. Plombon, E. Andideh, V.M. Dubin, J. Maiz, Influence of phonon, geometry, impurity, and grain size on copper line resistivity, Appl. Phys. Lett. 89 (2006) 113124, , https://doi.org/10.1063/1.2355435.
[39] M.J. Kim, T. Lim, K.J. Park, O.J. Kwon, S.-K. Kim, J.J. Kim, Characteristics of pulse-reverse electrodeposited Cu thin film: II. Effects of organic additives, J. Electrochem. Soc. 159 (2012) D544–D548, https://doi.org/10.1149/2.046209jes.
[40] N. Lazarus, C.D. Meyer, Stretchable inductor with liquid magnetic core, Mater. Res. Express 3 (2016) 036103, , https://doi.org/10.1088/2053-1591/3/3/036103.
[41] L.F. Arenas, F.C. Walsh, C. Ponce de León, 3D-printing of redox flow batteries for energy storage: a rapid prototyping laboratory cell, ECS J. Solid State Sci. Technol. 4 (2015) P3080–P3085, https://doi.org/10.1149/2.0141504jss.
[42] F.C. Walsh, L.F. Arenas, C. Ponce de León, Developments in electrode design: structure, decoration and applications of electrodes for electrochemical technology, J. Chem. Technol. Biotechnol. 93 (2018) 3073–3090, https://doi.org/10.1002/jctb.5706.